Journal of Sol-Gel Science and Technology (2020) 94:582–595
https://doi.org/10.1007/s10971-019-05185-y

ORIGINAL PAPER: SOL-GEL AND HYBRID MATERIALS FOR ENERGY, ENVIRONMENT AND BUILDING APPLICATIONS

Check for updates

Synthesis of novel MTF aerogels with adsorption performance

Q. I. Zhen-Tao[1] · H. E. Fang[1]

Received: 8 June 2019 / Accepted: 5 November 2019 / Published online: 16 November 2019
© Springer Science+Business Media, LLC, part of Springer Nature 2019

Abstract

The designability of aerogels and the grafting capability of groups were used in this study. A novel type of aerogel based on melamine–formaldehyde (MF) aerogels was synthesized by introducing thiourea groups, and the changes in sol particle diameter, formation mechanism of wet gel, and gel time during the formation of wet gel were studied in detail. Laser particle size, Brunauer–Emmett–Teller, and Fourier transform infrared analyses were combined with scanning electron microscopy and other characterization methods. Results showed that the thiourea group was successfully introduced into the MF aerogels. The specific surface area of the melamine–thiourea–formaldehyde (MTF) aerogel was 439.3 m^2/g, and the average pore diameter was as high as 1.8 nm without losing the typical 3D spatial network structure and porous material properties of aerogels. The change in particle diameter in the gelation process was systematically revealed for the first time, and the gelation time of wet gel was shortened to 218 min. The properties of aerogel porous materials and the complexing capability of amino and thiourea groups with regard to noble metal ions were used to test the performance of MTF aerogels in the adsorption and selective adsorption of noble metal ions. The findings indicated that the adsorption capacity of MTF aerogel was 88 mg·g^{-1} and the adsorption capacity of the MTF resin was 63 mg·g^{-1}, and the adsorption value of aerogel increased by 39% compared with MTF resin. In the selective adsorption experiment, the uptake values of MTF aerogel were found as 57.5 mg Ag^{+}·g^{-1}, 6.1 mg Cu^{2+}·g^{-1}, and 3.6 mg Zn^{2+}·g^{-1}. And the selective adsorption values of MTF resin were 16.3 mg Ag^{+}·g^{-1}, 0.1 mg Cu^{2+}·g^{-1}, and 0.05 mg Zn^{2+}·g^{-1}. The results show that the adsorption and selective adsorption capacity of MTF aerogel to silver (I) ions was higher than MTF resin. It was seen that the MTF aerogel prepared in this study has a large specific surface area, uniform pore size distribution, and strong adsorption and selective adsorption capacity for noble metals. It provides a new method for the selective adsorption of noble metal ions. The preparation of the aerogel is also simple and quick and entails a short gelation time and low cost.

Supplementary information The online version of this article (https://doi.org/10.1007/s10971-019-05185-y) contains supplementary material, which is available to authorized users.

✉ H. E. Fang
hefang@haut.edu.cn

[1] Department of Material Science and Engineering, Henan University of Technology, Zhengzhou 450007, China

Graphical Abstract

The formation mechanism of MTF aerogels was revealed, meanwhile, comparing before and after the adsorption and selective adsorption of precious metal ions by MTF aerogel, it can be confirmed that the MTF aerogel was successfully synthesized and possessed better adsorption and selective adsorption for precious metal ions.

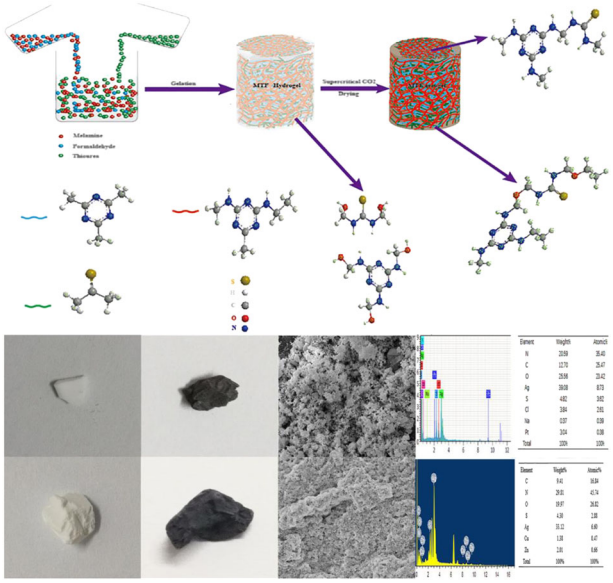

Highlights

- The melamine-thiourea-formaldehyde (MTF) aerogel containing thiourea group was fabricated.
- The gelation time of wet gel was shortened to 218 min.
- The MTF aerogels possess high specific surface area (439.3 m^2/g) and total pire volume (2.3 cm^3/g).
- The adsorption and selective adsorption values of MTF aerogels on silver (I) ions were 88 $mg{\cdot}g^{-1}$ and 57.5 $mg{\cdot}g^{-1}$, respectively, which were higher than that of resins.

Keywords Sol–gel · MTF aerogel · Reaction mechanism · Gelation time · Adsorption and selective adsorption capacity

1 Introduction

Porous solid nanomaterial aerogels have superior physical and chemical properties [1], such as large surface area [2], high porosity, low dielectric property [3], low density [4], low thermal conductivity [5], specific acoustic properties, and high adsorption performance. Therefore, aerogels are widely applied in matrices for active substances, extracellular scaffolds, energy storage, sensor materials, catalysis, automobile manufacturing, spacecraft, skyscrapers, electronic devices, clothing, and other areas [6–9]. However, the current cost of aerogels is higher than that of other traditional materials. Therefore, extensive effort has been exerted to reduce their manufacturing cost and thus enable them to become globally widespread.

Aerogels are created by forming a 3D wet gel network and removing the solvent without pore collapse and shrinkage. Aerogels can be prepared through the sol–gel process and supercritical fluid drying from inorganic or organic precursors. The most widely used organic compounds for aerogel synthesis are resorcinol–formaldehyde and melamine–formaldehyde (MF), which are synthetic polymers. MF has outstanding application performance and has been studied in past decades. Ruben et al. [10] prepared an MF aerogel with a density of 100–200 mg/cm^3, and the specific surface area was 800–900 m^2/g. Nguyen et al. [11] studied the effects of preparation parameters (gelation temperature and solution pH) on MF aerogel formation, and the gelation time was one week. However, the gelation time was long in their work. If MF aerogel can be prepared and controlled within a short gelation time, then the preparation cost of aerogels will be considerably reduced. The introduction of an appropriate thiourea group to the sol–gel system may also shorten the gelation time. During the experiment in the study of Nguyen et al., the gelation time was not more than 30 h when an appropriate thiourea group was introduced. Aerogels are porous materials with a large specific surface area and excellent adsorption performance. By using the designability of organic aerogels, adsorption of noble metal ions can be achieved through the introduction of certain groups into the aerogel skeleton. It is chelated with several functional groups with N, O, S, and P as atom

donors. These functional groups can form coordination complexes with different metal ions, which is one of the effective ways to capture metal ions [12]. The aerogel prepared by Klonkowski et al. [13] is likely to be chemically adsorbed on Cu (II) ions by combining with (3-aminopropyl) trimethoxysilane and (3-(2-aminoethyl) amidopropyl) trimethoxysilane and fixing them to the surface and internal parts of xerogels. Motahari et al. [14] developed amino-modified resorcinol formaldehyde aerogels to capture Pb (II), Hg (II), and Cd (II) ions from aqueous solutions. They studied the effects of changes in several adsorption parameters, such as temperature, pH, contact time, adsorbent concentration, and initial metal concentration, on adsorption capacity. The results showed that the adsorption process is entirely determined by pH, and the maximum adsorption capacities of Pb (II), Hg (II), and Cd (II) metal ions are 156.3 and 151.5 mg/g at pH values of 6 and 5, respectively, in an hour. This result is attributed to the formation of complexes between metal ions and surface amino groups acting as adsorption mechanisms for ions on the aerogel surface. Biyao Gao et al. [15] fabricated a thiol-functionalized nanocellulose aerogel-type adsorbent for the efficient capture of Hg(II) ions through facile freeze-drying of bamboo-derived 2,2,6,6-tetramethylpiperidine-1-oxyl oxidized nanofibrillated cellulose suspension in the presence of hydrolyzed 3-mercaptopropyltrimethoxysilane sols. The modified aerogel effectively and selectively removed more than 92% of Hg (II), and the maximal adsorption capacity was as high as 718.5 mg/g. Therefore, novel aerogels could be prepared through the sol–gel process and with melamine, thiourea, and formaldehyde as raw materials. These aerogels are expected to exhibit good adsorption properties for noble metal ions. Previous research has revealed that thiourea-containing resins have definite selective adsorption for precious metal ions, but they demonstrate certain limitations in adsorption capacity and speed. Therefore, making melamine–thiourea–formaldehyde (MTF) into aerogels and further study of the formation of MTF aerogels are crucial. The formation mechanism of wet gel and the factors that affect the microstructure and surface area of aerogels are important.

In the present study, we comprehensively described a simple method of producing MTF aerogels. The purpose was to produce novel aerogels that have a certain adsorption property for noble metal ions and analyze their structural characteristics. The effects of thiourea/MF mass ratio, reactant concentration, temperature, and pH on aerogel gelation time were discussed in detail. The structure and properties of aerogels were evaluated with necessary characterization equipment.

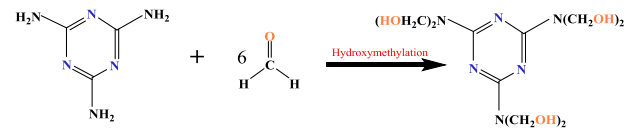

Scheme 1 MF (1:6) hydroxymethylation

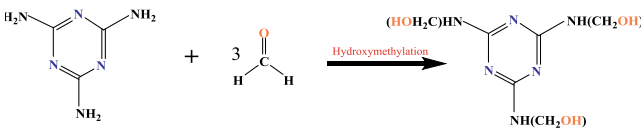

Scheme 2 MF (1:3) hydroxymethylation

Scheme 3 TF (1:2) hydroxymethylation

2 Materials and experimental

2.1 Chemicals

The chemical reagents used in the experiment were as follows. The thiourea power was bought from Tianjin Yongda Chemical Reagent Co., Ltd. Formaldehyde solution (36%), cyclohexane (99.8%), and ethanol (99.7%) were purchased from ChengDu Kelong Chemical Reagent Company. Melamine was supplied by Sigma-Aldrich Company, Ltd. CO_2 (99.9%) was purchased from MianYang Changjun Gases Co., Ltd., and silver nitrate, copper nitrate, zinc nitrate, Na_2CO_3 and hydrochloric acid were provided by Tianjin Dingshengxin Chemical Industry Co., Ltd. All regents and chemicals were used without further purification.

2.2 Preparation of MTF aerogels

MTF hydrogels were synthesized by hydroxymethylation (Schemes 1–3) and condensation (Schemes 4–6) reactions [16] and prepared with melamine, formaldehyde, and thiourea via a two-step sol–gel process. The formation and reaction mechanism of the MTF hydrogels are shown in Fig. 1. Melamine is a hexafunctional monomer that could react at each of the amine hydrogens. Under alkaline conditions, formaldehyde was added to the positions to form hydroxymethyl ($–CH_2OH$) groups, and the same reaction occurred in every amine hydrogen of the thiourea group to form hydroxymethyl ($–CH_2OH$) groups. In the second part of the polymerization, the solution was acidified to facilitate the condensation of the intermediates, resulting in the formation of gels. The main cross-linking reactions included the formation of the dehydration and condensation reaction between the hydroxyl group on the hydroxymethyl group and amino primary "H" linked to the amino group (Scheme 4, diamino

methylene–$NHCH_2NH$–), the dehydration condensation reaction between carboxyl groups on the hydroxymethyl group linked to the amino group (Scheme 5, methylene ether–$NHCH_2OCH_2NH$–), and the dehydration and condensation reaction between the hydroxyl group on the hydroxymethyl group and amino secondary "H" linked to the amino group (Scheme 6, diamino methylene–$NHCH_2NH$–) bridges. First, melamine, formaldehyde, and Na_2CO_3 (melamine: deionized water mass ratio = 1:10) were dissolved in deionized water under magnetic stirring at 95 °C and formed a translucent solution of melamine and formaldehyde [17]. Second, the prepared thiourea solution was added to the as-prepared translucent solution, while stirring and heating at 95 °C for about 30 min until the mixed solution was clear.

Scheme 4 polycondensation

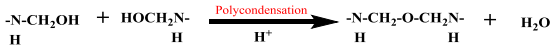

Scheme 5 polycondensation

Scheme 6 polycondensation

Third, the pH value was adjusted at ~1.5 by using an HCL solution (1 mol/L). In this process, the ratio of thiourea to (melamine and formaldehyde) mass was 0.05:1, and the mole ratio of melamine to formaldehyde was 1:3.7. Lastly, the solution was poured into glass weighing bottles and subsequently molded (mold with 25 mm diameter). The samples were stored at 95 °C for 2–20 h until gelation. The gelation process was stopped when the viscosity of the solution increased and basic liquidity disappeared. To make the skeleton structure solid, previously prepared wet gels were aged for 3 days at room temperature. Different solutions concentrations and processing parameters were used to obtain different hybrid gel samples.

The drying process of wet gel was divided into two steps. First, water was replaced with ethanol mixed with deionized water (the volume ratio of ethanol to deionized water was 1:2), ethanol, and acetone for 24 h, and the process was repeated three times. Second, the acetone-saturated hybrid gels were wrapped with gauze and placed in a high-pressure stainless steel autoclave with a volume of 1000 ml. Subsequently, the acetone-saturated hybrid gels were dried via supercritical CO_2 extraction at 40 °C and 8 MPa for 10 h, and the pressure was slowly released at a constant temperature of 40 °C. During sample removal, air was gradually replaced with CO_2, and aerogel samples were obtained successfully. The MTF

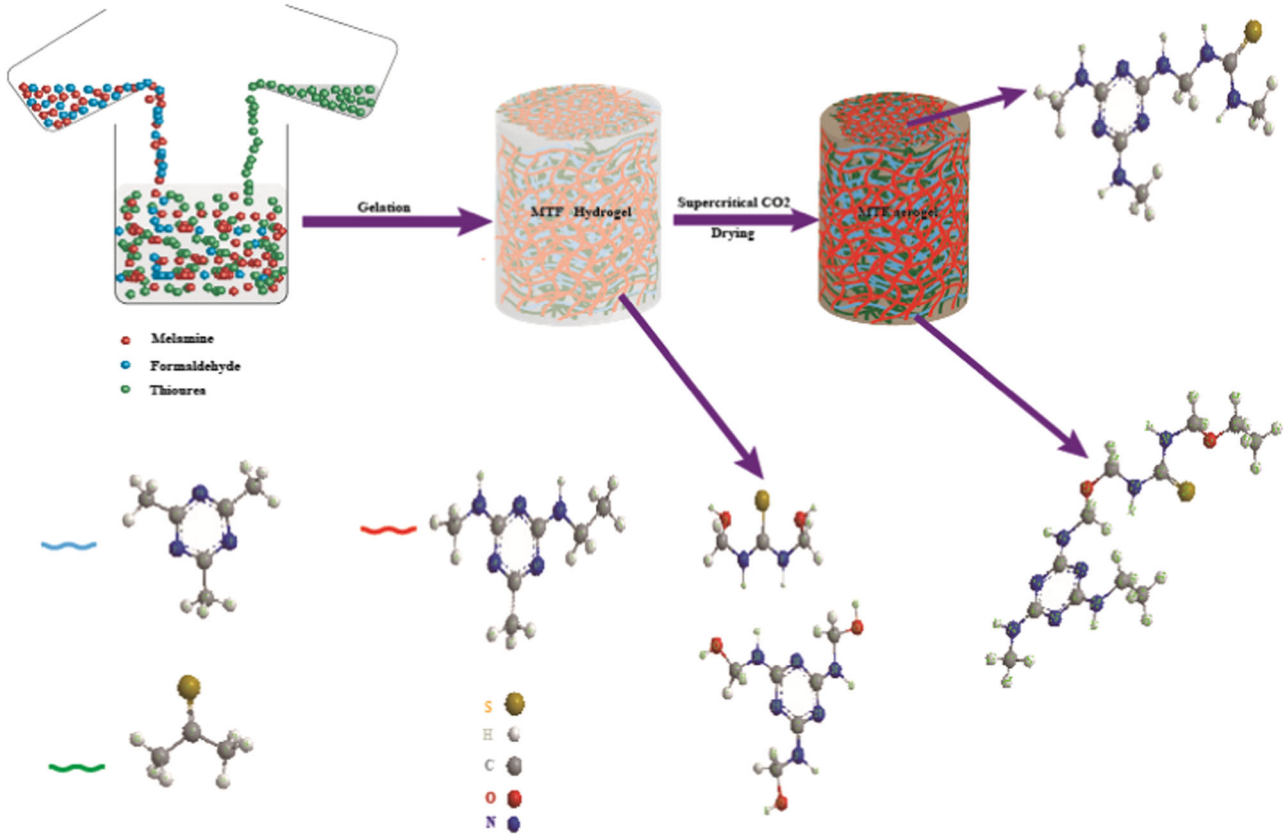

Fig. 1 Reaction mechanism of MTF hydrogels

aerogels with different thiourea/MF mass ratios were labeled as MTF1, MTF2, MTF3, and MTF4 with mass ratios of 0.05:1, 0.10:1, 0.15:1, and 0.20:1, respectively.

2.3 Characterization

The pore size distribution and specific surface of the aerogels were measured with the multipoint Brunauer–Emmett–Teller (BET) method on the basis of the nitrogen adsorption and desorption isotherms of nitrogen at 77 k using a Quantachrome instrument (America). The changes in sol particle diameter were characterized using a laser particle size analyzer (Microtrac S3000, USA). The microstructures and surface characteristics of the samples were observed through scanning electron microscopy (SEM; INSPECT F50, FEI). X-ray diffraction (XRD) analysis was also conducted with a MiniFlex300/600 instrument. The surface chemical properties of the samples were characterized by Fourier transform infrared spectroscopy (FT-IR), and FT-IR spectra of thin-slice samples were collected from 400 to 4000 cm^{-1} by using IRPESTIGE-21 after mixing with fully dried KBr at a ratio of 1:(15–50). An Agilent 5100 inductively coupled plasma atomic emission spectrum (ICP-AES) was used for the determination of metal ions in aqueous solutions before and after adsorption or elution.

2.4 Adsorption and selective adsorption experiments

In the adsorption experiments, 100 mg of MTF aerogel and 100 ml of Ag (I) ions solutions (initial concentration was 0.1 $mg{\cdot}mL^{-1}$) were added into a 250 ml stoppered conical flask, adjusted the pH values at about 3. In the experiments, keep stirring in a water bath at a constant temperature of 30 °C continue 120 min. In order to prove the selective adsorption properties of MTF aerogels on Ag^{+}, and the selective adsorption of Ag^{+} together with Cu^{2+} and Zn^{2+} metal ions was investigated. And in order to compare the adsorption and selective adsorption properties of MTF aerogels with MTF resins for silver (I) ions, and the adsorption and selective adsorption experiments of MTF resins were carried out under the same conditions as MTF aerogels. Then the mixed solution was filtered and the Ag^{+}, Cu^{2+}, and Zn^{2+} concentration in after filtered solution was measured by ICP-AES. The adsorption capacity (Q) was calculated using Eq. (1).

$$Q = (C_0 - C_e)\,V/Mm, \tag{1}$$

where Q is the adsorption capacity of aerogel, $mmol{\cdot}g^{-1}$; C_0 is the initial concentration of ions, $mg{\cdot}ml^{-1}$; C_e is the equilibrium concentration of after adsorption ions, $mg{\cdot}ml^{-1}$; V is the solution volume, ml; M is the molar mass of the metal ion, $g{\cdot}mol^{-1}$; m is the mass of the aerogel, g.

3 Results and discussions

3.1 Gelation time

The hexafunctional melamine, thiourea, and formaldehyde reacted under alkaline conditions to form a large number of hydroxymethyl (–CH_2OH) groups. In this process, (–NH_2^{+}–CH_2O^{-}) protons were transferred from active N to inert O, and dehydration occurred. After the hydroxymethylation process was completed, the superfluous base catalyst was neutralized with acid to dehydrate the hydroxymethylation reaction under the condition of acid catalysis. MTF aerogels with a 3D network structure were formed through dehydration, condensation, and cross-linking. Gelation time was mainly affected by the reactants (type, concentration, and ratio), conditions (pH and gel temperature), and other factors [18]. The relationship between gelation time and various factors is described in Fig. 2. The preliminary investigation showed that the gelation time of pure MF aerogels was long (2880 min), but adding a certain amount of the thiourea group helped shorten the gelation time. Therefore, studying the effect of thiourea addition on gel time is crucial. As shown in Fig. 2b, when the mass ratio of thiourea/MF was 0.05:1, the gelation time was shortened to 218 min, and the gelation process of the MTF aerogels was much faster than that of the pure MF aerogel. The introduction of thiourea accelerated the process of hydroxymethylation and increased the nucleation rate of MF particles, thus shortening the gelation time. In addition, when the mass ratio of thiourea/MF gradually increased, the gelation process of the MTF aerogels gradually slowed down due to the dominant factor of melamine in the gelation process. When the total mass concentration was unchanged, the proportion of melamine decreased with the increase in thiourea, thus increasing the total gelation time. Figure 2a, d show that the gelation time decreased with the increase in the total mass concentration and temperature of the reactants. Figure 2c indicates that the gelation time of the MTF aerogels increased gradually with the increase in pH value from 1.0 to 3.0. Previous literature has reported that solution pH is the main variable that controls the gelation time, structure, and properties of MF aerogels. However, the content of melamine was relatively large in this research system; therefore, the reaction rate of the system depended mainly on the reaction rate of MF, and an appropriate reduction in acidity and alkalinity can increase the reaction rate of melamine. Therefore, the gelation time of the MTF aerogels decreased with the decrease in pH.

3.2 Laser particle size analysis

Complex reactions, including condensation, formation of small and large clusters, and final formation of the 3D skeleton structure, were observed in the process of gelation. Representative time points within 30–180 min were selected

in the laser particle size experiments for detailed analysis to clearly reflect the changing process of particle size distribution at different times. At the initial time of 30 min (Fig. 3a), a large number of clusters with particle sizes ranging from 0.3 to 2.8 μm existed in the sol system, and many of clusters had a size of ~383.9 μm, which indicated

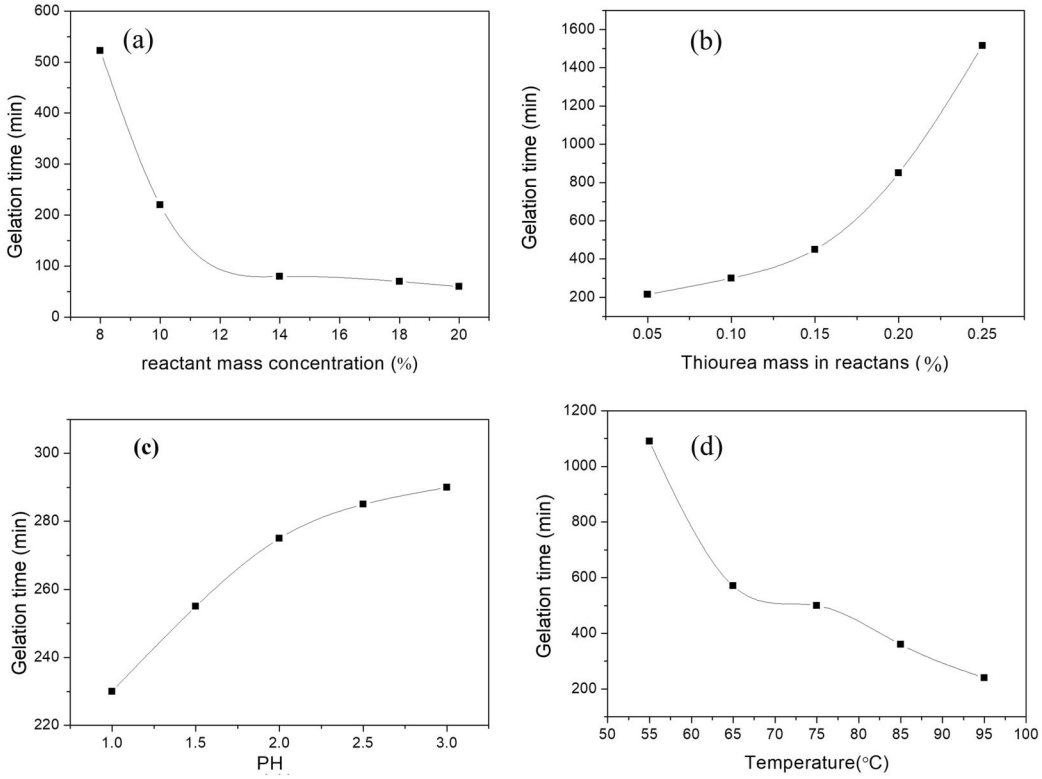

Fig. 2 Relationship between gelation time and reactant mass concentration (**a**) thiourea/MF mass ratio (**b**), pH, (**c**) and temperature (**d**)

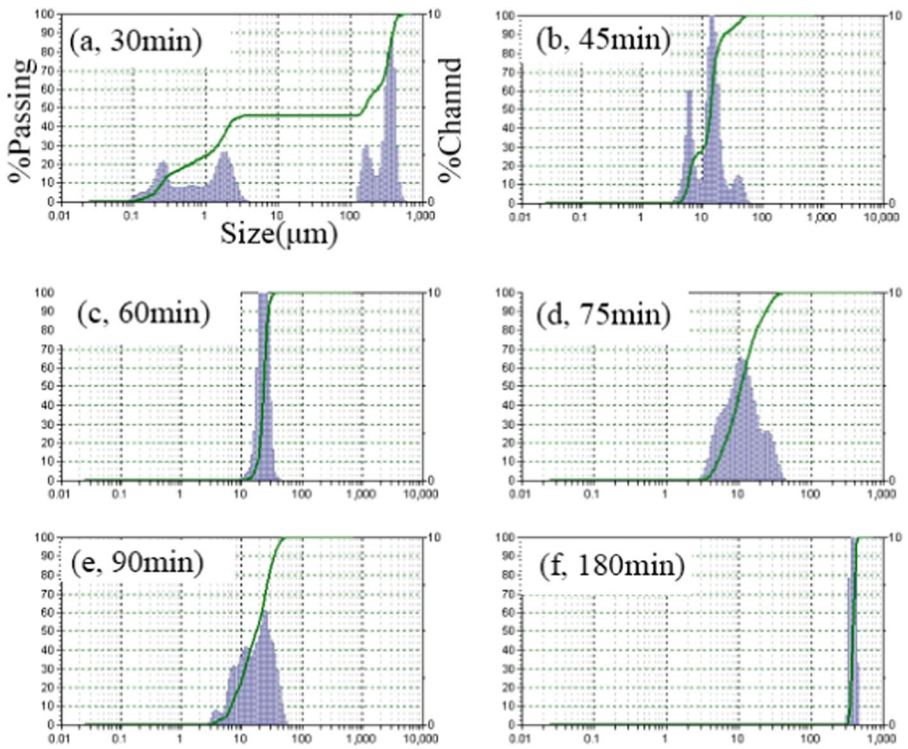

Fig. 3 Particle size distribution of precursors during gelation at different times

the errors caused by the failure to separate the entire gel in time during the testing process. When gelation was carried out at 45 min (Fig. 3b), the particle size of the sol particles ranged from 5.0 to 9.3 and 11.0 to 4.0 μm, indicating that the particles were combined into large clusters in the reaction process. The particle sizes at 60, 75, and 90 min are shown in Fig. 3c–e, respectively. Only a small change was observed compared with Fig. 3b, but it was clear that the particle sizes in the reaction process of 45–75 min showed an increasing trend, indicating that the process of small particles combining with each other to form large clusters still took place. Figure 3f shows the particle size distribution in the reaction at 180 min. A large number of particles had sizes of 352–497.8 μm in the system. The viscosity of the sol was high, indicating that the sol had reached a gel-like state and that the sol had formed gelation afterward. The specific values of the particle size distribution of precursors during gelation at different times are given in Table 1.

The laser particle size distribution shows the growth and condensation of MTF aerogels and the specific process, which includes the process of reactant monomer condensation, microparticles, small clusters, large clusters, and gels.

3.3 BET analysis

As shown in Fig. 4, the specific surface area, variation in pore size, and pore size distribution of the samples were measured using nitrogen adsorption/desorption isotherms at 77.35 K. The profile of the adsorption/desorption isotherms indicated that the MTF aerogels presented a continuous network of pores with a size ranging from microporous to macroporous domains, as illustrated in Fig. 4a–e, indicating an essentially multihole structured material. According to the IUPAC standard adsorption isotherm, the isotherms roughly shown in Fig. 4a–e can be classified as type IV. However, the diagrams in Fig. 4a–e conform to the type I standard isothermal curve in the region of relatively low pressure, and the gas adsorption capacity showed rapid growth due to the micropore filling process. With the continuation of adsorption, the slope of the curve decreased gradually, indicating that the microporous adsorption was full and microporous adsorption was nearly saturated. The adsorption continued as the relative pressure increased. At this time, the adsorption isotherm curve conformed to type IV, and finite multilayer adsorption was formed. In the area with relatively high pressure, capillary agglomeration of the adsorbate occurred, and the isothermal curve rose rapidly. When all the pores were condensed, adsorption only occurred on the outer surface, which was far smaller than the inner surface area, and the curve was flat. When the relative pressure was close to 1.0, the adsorption curve showed an upward trend on the macropores. Hysteresis loops were observed in this region due to the condensation of capillaries, and the isotherms obtained during desorption did not coincide with those obtained during adsorption. The desorption isotherms were higher than the adsorption isotherms, which resulted in adsorption hysteresis, and presented H3 hysteresis loops. This result indicates that a certain amount of mesopores existed in the aerogel samples. The starting point of the hysteretic loop was around 0.7 of relative pressure, which reveals large pores in the aerogel samples or large pores formed by the accumulation of particles. Figure 4a–e show a large number of micropores and a certain number of mesopores in the aerogel samples, which was verified by the pore size distribution. As shown in Fig. 4f, the pores of five samples were all mesopores and micropores, but the pore sizes were mainly distributed at 1–16 nm.

The pore structural parameters of the MTF aerogels are given in Table 2. S_{BET}, V_t, and average pore diameter reached the maximum when the thiourea/MF mass ratio decreased from 0.25:1 to 0.05:1. The S_{BET} and mesoporosity of the MTF aerogels could be significantly improved by selecting an appropriate thiourea/MF mass ratio (0.05:1). MTF1 had the largest specific surface area (439.3 m^2/g) and ideal pore volume (2.3 cm^3/g) with an average pore diameter of about 1.9 nm, as clearly shown in Fig. 5a. Several previously formed mesopores were blocked or broken due to the prolonged gelation time and gel shrinkage during solvent exchange and supercritical CO_2 drying, which resulted in a decrease in BET specific surface area and pore volume. The mass ratio of thiourea/MF evidently influenced the specific surface area and pore volume, and MTF1 had the most appropriate pore diameter and size distribution.

On the basis of the analysis of the specific surface area of the samples, MTF1 with the largest specific area was selected for the adsorption test, and MTF1 after Ag^+ adsorption was characterized via SEM and energy-dispersive X-ray spectroscopy (EDS). To better prove the adsorption capacity of the samples, samples of MTF1 before and after Ag^+ adsorption were analyzed via FT-IR.

Table 1 Particle size distribution of precursors during gelation at different times

Gelation time	Particle size distribution
30 min	0.2–0.5 μm, 1.4–2.8 μm
45 min	5.0–9.3 μm, 11.0–24.0 μm
60 min	15.6–28.5 μm
75 min	4.8–31.1 μm
90 min	15.6–48.0 μm
180 min	352.0–497.8 μm

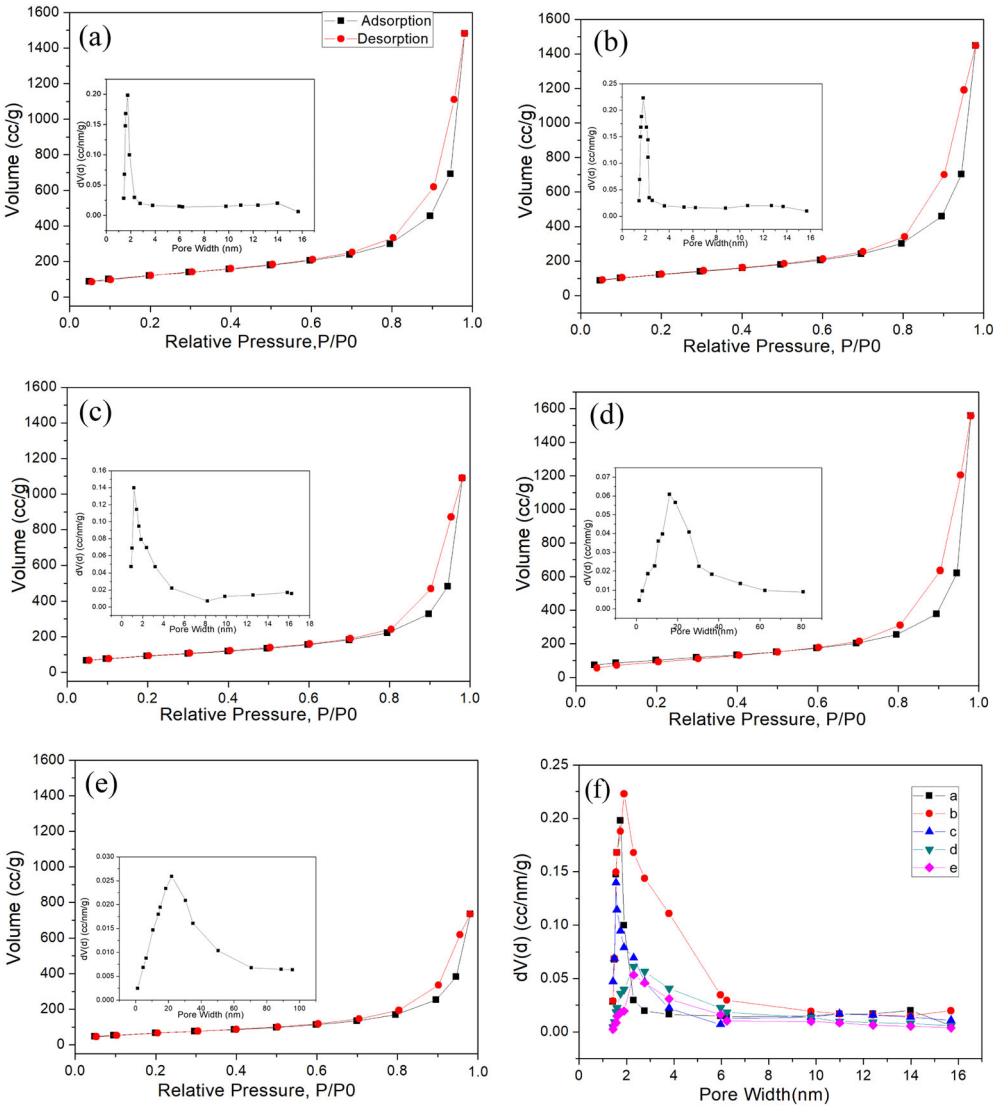

Fig. 4 Nitrogen adsorption/desorption isotherms at 77.35k and BJH analysis (inset) of pore size distributions of the MTF1 aerogels (**a**), MTF2 (**b**), MTF3 (**c**), MTF4 (**d**), MTF5 (**e**), and detailed view of the pore size distribution curves (**f**)

Table 2 BET surface characterization of MTF aerogels

Experimental parameters	Surface area (m^2/g)[a]	Total pore volume (cm^3/g)[b]	Average pore diameter (nm)[c]
MTF1	439.3	2.3	1.9
MTF2	438.9	2.3	1.8
MTF3	375.1	2.5	1.6
MTF4	370.4	1.7	1.4
MTF5	283.2	1.2	1.3

[a]The surface area is obtained by BET calculation [18]

[b]The total pore volume is the single point adsorption total pore volume of pores with <130 nm diameter at $P/P0 = 0.98$

[c]The average pore diameter is estimated with the 4 V_T/A method. V_T is total pore volume

3.4 SEM morphology

The morphologies and structures of the MTF aerogels were elucidated via SEM observation. SEM images of the MTF aerogels are shown in Fig. 5a–e. Typical organic clusters with a 3D skeleton structure are clearly visible in Fig. 5a–e, and a large number of pores exist on the surface of the sample. The results revealed that melamine and thiourea were evenly mixed with formaldehyde and formed a homogeneous porous structure in the MTF aerogels. When the mass ratio of thiourea/MF increased from 0.05 to 0.25, the SEM images of the MTF aerogels exhibited significant changes in morphology and structure, as shown in Fig. 5a–e. Figure 5a–c show the skeleton structure composed of melamine and the pores between the

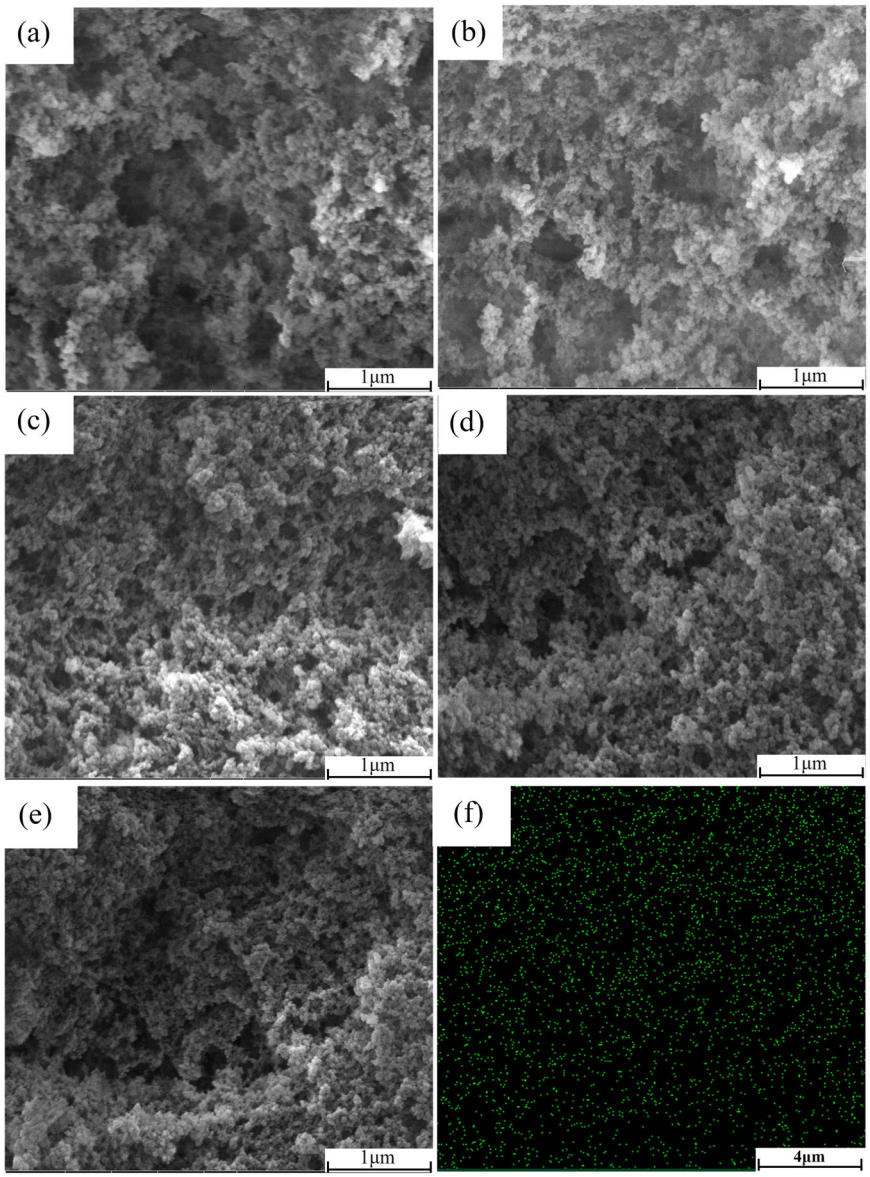

Fig. 5 SEM images of MTF1 (**a**), MTF2 (**b**), MTF3 (**c**), MTF4 (**d**), MTF5 (**e**), and surface distribution chart of S element obtained by EDS for MTF1 (**f**)

melamine structures. When the amount of thiourea mass was small, numerous pores and larger pore diameters were observed. With the increase in the amount of thiourea mass, the structure was gradually compacted, the pores decreased, and the pore diameter decreased, as reflected in the BET value. The surface area, total pore volume, and average pore value decreased with the increase in the amount of thiourea added. However, as shown in Fig. 5d, e, the skeleton structure became increasingly dense and tight with the increase in thiourea mass. The previously formed mesopores and pore channels might be partially blocked by the MTF clusters in the melamine matrix. According to Fig. 5f, the nitrogen element (green point) was distributed uniformly in the aerogels and without an obvious aggregation phenomenon. Therefore, the hybrid aerogel had a uniform structure. This phenomenon fully explains the typical aerogel structure of the samples and indicates that the samples were successfully prepared and effective. At the initial stage of gel formation, melamine and thiourea were hydroxymethylated, followed by a dehydration–condensation–cross-linking reaction. Eventually, the MTF aerogels were formed. Melamine is a triazine-containing heterocyclic ring, which is a rigid structure that can be used as a skeleton structure in MTF aerogels. With the addition of thiourea, hydroxymethylation may extend the branched chain and improve the degree of chain crosslinking. Subsequently, dehydration, condensation, and crosslinking were executed to form a compact structure, which further made the skeleton structure dense and tight.

3.5 X-ray diffraction (XRD) phase composition analysis

Figure 6 shows wide-angle XRD patterns of the MTF1, MTF2, MTF3, MTF4, and MTF5 aerogels. The main diffractive regions in the MTF aerogels were at 23.44° with the highest peak intensity. The XRD patterns show very broad lines, indicating that the MTF aerogel is a typical non-crystalline material.

3.6 FT-IR spectra analysis

The obtained MTF aerogels were characterized by FT-IR analysis, and the FT-IR spectra of the MTF aerogels are shown in Fig. 7. The typical C–H stretching absorption of the methylene peak around 2933 cm^{-1} is given in Fig. 7. The FT-IR spectrum of melamine showed typical respiratory patterns of triazine rings at 813 and 1550–1437 cm^{-1} regions, whereas that of thiourea showed the C=S stretching vibration of thiourea at 1427 and 1092 cm^{-1} regions. The characteristic FT-IR absorption band of the MTF aerogels at 1548 cm^{-1} was used as the thiourea functional group. Additionally, the N–H stretching vibration of melamine and thiourea was observed in the 3500–3100 cm^{-1} region, and the area of 1108 cm^{-1} was assigned to C–O–C, indicating that the thiourea groups played an important role in the reaction. The N and S donor atoms on the surface of aerogel particles were effectively adsorbed due to the incomplete release of oxygen. Subsequently, the typical structure of aerogels was verified by FT-IR analysis. The

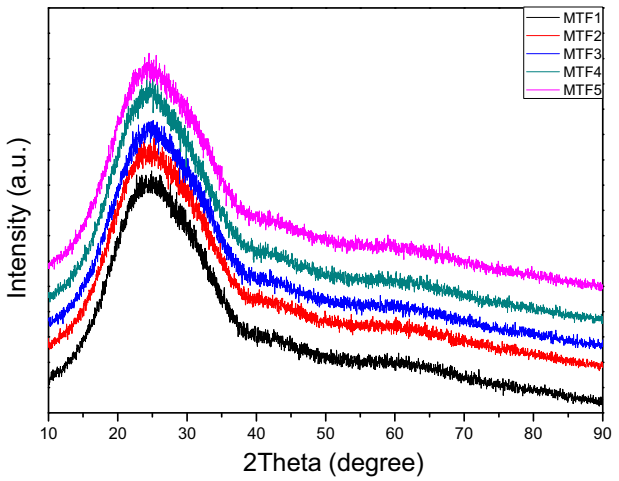

Fig. 6 XRD patterns of the MTF1, MTF2, MTF3, MTF4, and MTF5 aerogels

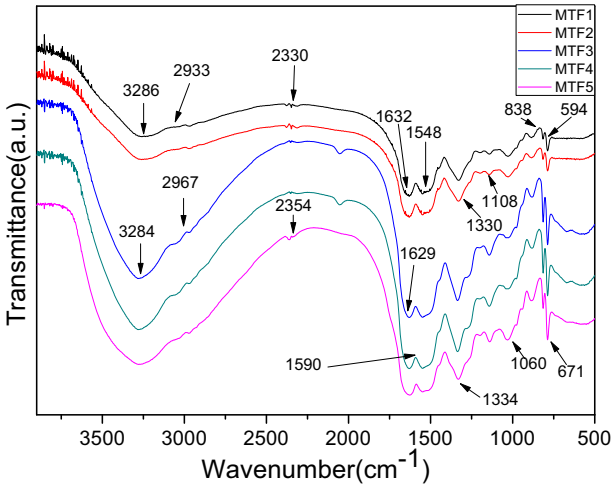

Fig. 7 FT-IR spectra of the MTF1, MTF2, MTF3, MTF4, and MTF5 aerogels

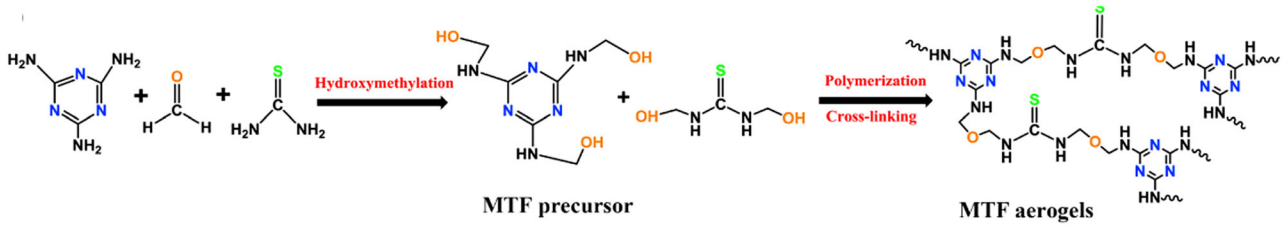

Fig. 8 Reaction equation of the MTF aerogel

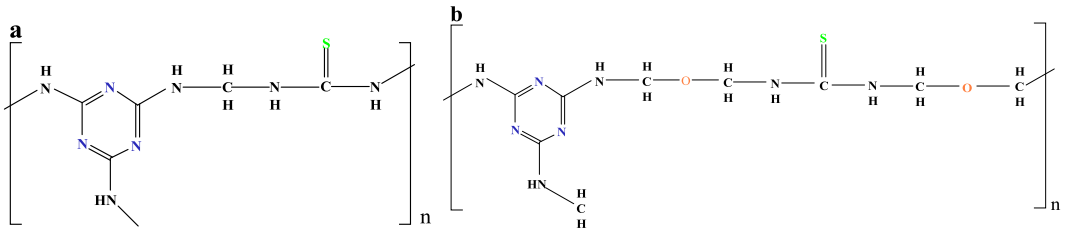

Fig. 9 MTF aerogel

corresponding MTF aerogel reaction equation and structure are shown in Figs 8, 9, respectively [19–21].

3.7 Adsorption and selective adsorption performance

According to the characteristics of MTF aerogel porous materials and the thiourea groups contained in them, MTF possesses high adsorption capacity and selective adsorption for precious metal ions. To verify this claim, there were two sets of experiments were conducted. On the one hand, the adsorption capacity experiment of MTF aerogel to silver (I) ions was tested by only containing Ag^+ in the solution. On the other hand, the selective adsorption capacity experiment of aerogel was investigated by mixing Ag^+ with Cu^{2+} and Zn^{2+} ions in the solution. The adsorption and selective adsorption capacity of MTF resin to silver (I) ions were obtained by using the same experimental scheme as MTF aerogel, and the experimental results were compared with MTF aerogel. The aerogels obtained from the MTF1 parameters were used for the adsorption experiments due to the large specific surface area and porosity of the aerogels obtained from these parameters; moreover, these properties have already been obtained in the characterization experiments. It was found that the MTF aerogel had silver (I) adsorption as 0.8 $mmol{\cdot}g^{-1}$ or 88 $mg{\cdot}g^{-1}$ and the adsorption capacity of resin was 0.6 $mmol{\cdot}g^{-1}$ or 63 $mg{\cdot}g^{-1}$ in Fig. S1, and the adsorption value of MTF aerogel increased by 39% compared with MTF resin. And the adsorption value of MTF aerogel was also higher than reported in previous literature [22] that the adsorption value of resin was 0.6 $mmol{\cdot}g^{-1}$ or 60 $mg{\cdot}g^{-1}$, and the adsorption value of MTF aerogel increased by 47% compared with the resin. The selective adsorption of MTF aerogels to silver (I) ions were shown in Fig. S2, the uptake values of MTF aerogel were found as 0.5 $mmol{\cdot}g^{-1}$ or 58 mg $Ag^+{\cdot}g^{-1}$, 0.09 $mmol{\cdot}g^{-1}$ or 6.1 mg $Cu^{2+}{\cdot}g^{-1}$ and 0.05 $mmol{\cdot}g^{-1}$ or 3.6 mg $Zn^{2+}{\cdot}g^{-1}$. And the selective adsorption of MTF resins to silver (I) ions were shown in Fig. S3, the adsorption values of MTF resin were 0.2 $mmol{\cdot}g^{-1}$ or 16 mg $Ag^+{\cdot}g^{-1}$, 0.002 $mmol{\cdot}g^{-1}$ or 0.1 mg $Cu^{2+}{\cdot}g^{-1}$ and 0.0008 $mmol{\cdot}g^{-1}$ or 0.05 mg $Zn^{2+}{\cdot}g^{-1}$. It was seen that MTF aerogel showed a higher uptake for silver (I) ions than the other ions at the same initial concentration as 0.1 mg/ml, and higher adsorption and selective adsorption capacity than MTF resin. The morphology of aerogels adsorbing and selective adsorbing Ag+ are shown in Fig. 10 and Fig. S4. The macroscopic morphologies before and after adsorption and selective adsorption Ag^+ are shown in Fig. 10a, b, Fig. S4a, b respectively. The aerogel were milky white, and after adsorption and selective adsorption of Ag^+, the color of the aerogel changed from milky white to black brown, indicating that Ag^+ was successfully adsorbed. To verify the microstructures of aerogels after adsorption, the SEM morphology was used to characterize the aerogel after Ag^+ absorption and selective adsorption. The surface in Fig. 10c and Fig. S4(c) were obviously covered with a layer of light-colored honeycomb material, which can be determined as the successful adsorption of gravity, and the content are high. The corresponding higher magnification SEM image are shown in Fig. 10d and Fig. S4d to further verify the capability of aerogels to adsorb and selective adsorb Ag^+. The pores on the aerogel surface were successfully coated with Ag^+. The adsorption of Ag^+ on the surface of or inside the MTF aerogels may depend on the electrostatic trapping or complexing capability of surface electrons. To confirm the elemental composition of the sample, element analysis of EDS was conducted, and the red coil was used as the point of departure. The element content showed that a large number of Ag elements existed in Fig. 10, and the atomic weight was 8.7%. It was found that relatively few of Ag elements existed in Fig. S4, and the atomic weight was 6.6%. At the same time, Cu and Zn elements appeared in Fig. S4, which indicated that MTF aerogels also adsorbed a small amount of Cu^{2+} and Zn^{2+}. These results indicate that the aerogel material prepared under these conditions had good adsorption and selective capacity for silver ions. The elements of Na, Cl, and Pt in the EDS analysis were caused by the adjustment of pH in the preparation process and the injection of Pt element in the SEM test to enhance conductivity.

3.8 FT-IR analysis after Ag^+ adsorption

The FT-IR spectra of the MTF aerogels after the adsorption of Ag^+ are shown in Fig. 11. The peaks of FT-IR spectra after the aerogels adsorbed Ag^+ exhibited corresponding changes. The FT-IR spectra of the aerogels after Ag^+ adsorption were compared with the infrared spectra, and the results show that the stretching vibration absorption peaks of N–H and C–N moved to the high wave direction. At the same time, the stretching vibration absorption peaks of C=O and N–C–N moved toward the low wave direction, the symmetrical stretching vibration absorption peak of C–O–C moved toward the high wave direction, and the antisymmetrical vibration absorption peak of C–O–C moved toward the low wave direction. After the adsorption of Ag^+, the stretching vibration absorption peak of C=S weakened near 1041 cm^{-1} and moved toward the low wave direction at 1037 cm^{-1}. In the vicinity of 1330 cm^{-1}, the adsorption peak of aerogel was not obvious before Ag^+ adsorption, and the peak appeared after Ag^+ adsorption. Compared with the situation before

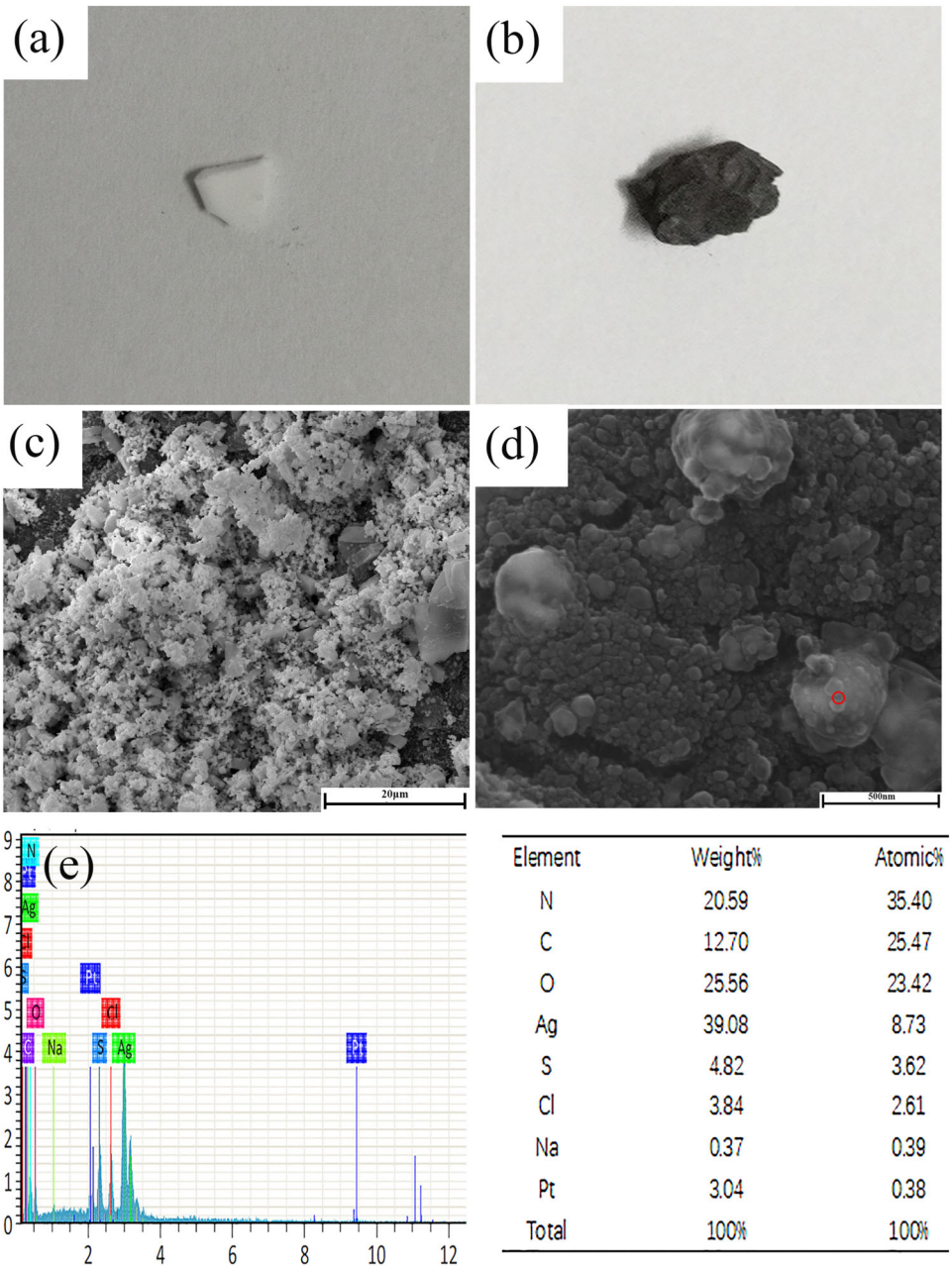

Element	Weight%	Atomic%
N	20.59	35.40
C	12.70	25.47
O	25.56	23.42
Ag	39.08	8.73
S	4.82	3.62
Cl	3.84	2.61
Na	0.37	0.39
Pt	3.04	0.38
Total	100%	100%

Fig. 10 Macroscopic comparison of MTF aerogels before and after adsorption (**a**, **b**). SEM images of the aerogel after Ag^+ adsorption under different experiment parameters (**c**, **d**). EDX element analysis spectrum of the MTF1 aerogel after the adsorption of Ag^+ ions (**e**)

adsorption, the aerogels coordinated with the noble metal ions after adsorption, and the atoms of the aerogels that participated in coordination reaction were S, N, and O.

4 Conclusions

A novel type of MTF aerogels was successfully prepared with sol–gel and supercritical drying methods by introducing a thiourea group into existing aerogels and using the structural designability and grafting capability of aerogel functional groups. The effects of T/MF ratio, pH, and reactant concentration on the gelation time of aerogels were investigated through experiments. BET, SEM, XRD, FT-IR, and laser particle size analysis were conducted to examine the properties of the aerogels before and after Ag^+ adsorption.

Analysis of the influencing factors of gel time revealed that the shortest gelation time was 218 min. The MTF1 aerogel with a thiourea/MF mass ratio of 0.05 had micropores with a large surface area (439.3 m^2/g) and ordered mesopores with a uniform pore size (1.7 nm) and pore volume (1.9 nm). Therefore, MTF1 possessed excellent features. Laser particle size analysis revealed the condensation, formation of small and large clusters, and final formation of a 3D skeleton structure. The preparation process and reaction mechanism of the MTF hydrogels were described in detail. The SEM

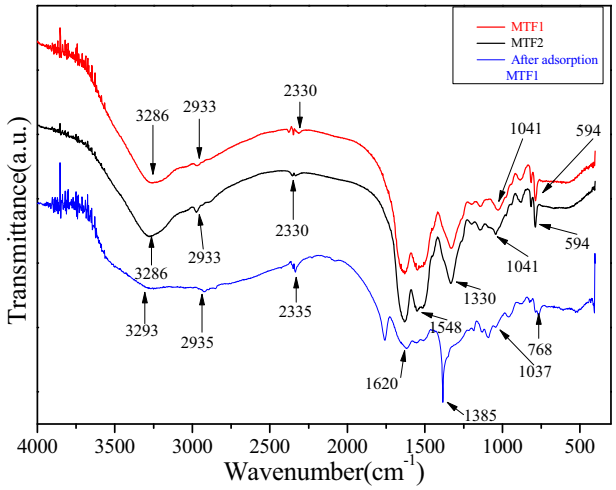

Fig. 11 FT-IR spectra of MTF1, MTF2, and after MTF1 Ag^{+} adsorption

morphology, XRD patterns, and FT-IR studies showed that MTF aerogels are typical amorphous structure materials with a 3D skeleton structure through hydroxymethylation, polycondensation, and cross-linking of melamine, thiourea, and formaldehyde. According to the characteristics of the MTF aerogel porous materials and the thiourea groups contained in them, MTF possesses high adsorption and selective adsorption capacity for precious metal ions. To verify this claim, the adsorption experiments were conducted with Ag^{+} and the selective adsorption of Ag^{+} together with Cu^{2+} and Zn^{2+} were investigated. Results showed that the adsorption capacity of MTF aerogels to silver (I) ions was 88 $mg{\cdot}g^{-1}$, and the adsorption capacity of MTF resin was 63 $mg{\cdot}g^{-1}$, and the adsorption value of aerogels increased by 39% compared with resins. In the selective adsorption experiment, the uptake values of MTF aerogel were found as 57.5 mg $Ag^{+}{\cdot}g^{-1}$, 6.1 mg $Cu^{2+}{\cdot}g^{-1}$, and 3.6 mg $Zn^{2+}{\cdot}g^{-1}$. It was seen that the MTF aerogel showed a higher uptake for silver (I) ions than the other ions at the same initial concentration, and higher adsorption and selective adsorption capacity than MTF resin. So the MTF aerogel prepared in this study has strong adsorption and selective adsorption capacity for silver (I) ions. The aerogels after Ag^{+} adsorption were characterized by SEM, EDS, and FT-IR. When the aerogels absorbed Ag^{+}, the SEM image showed that the aerogels' surface adsorption had a large amount of Ag. Moreover, the micropores of the aerogels captured plenty of Ag^{+}. EDS element analysis revealed that the Ag element had a large atomic ratio, indicating that the MTF aerogels had good Ag^{+} adsorption and selective properties. Therefore, MTF aerogels also exhibit a highly selective adsorption performance for other noble metal ions.

Acknowledgements We are grateful to Henan University of Technology. This study was financially supported by the Natural Science Project of Science and Technology Department of Henan Province (No. 182300410181) and the Project of "Special Funds for Basic Scientific Research Business Expenses of Provincial Universities" of Henan University of Technology (No. 2018RCJH02).

Compliance with ethical standards

Conflict of interest The authors declare that they have no conflict of interest.

Publisher's note Springer Nature remains neutral with regard to jurisdictional claims in published maps and institutional affiliations.

References

1. Pierre AC, Pajonk GM (2002) Chemistry of aerogels and their applications. Chem Rev 34(4):4243–4265
2. Gurav JL, In-Keun J, Hyung-Ho P, Kang ES, Nadargi DY (2010) Silica aerogel: synthesis and applications. J Nanomater 2010 (24):1–11
3. Hrubesh LW, Keene LE, Latorre VR (1993) Dielectric properties of aerogels. J Mater Res 8(7):1736–1741
4. Hrubesh LW (2010) ChemInform abstract: aerogels: the world's lightest solids. Cheminform 22(13)
5. Kistler SS, Caldwell AG (2002) Thermal conductivity of silica aërogel. Indengchem 26(6):658–662
6. Hrubesh LW (1998) Aerogel applications. J Noncryst Solids 225 (1):335–342
7. Chin SF, Romainor ANB, Pang SC (2014) Fabrication of hydrophobic and magnetic cellulose aerogel with high oil absorption capacity. Mater Lett 115(2):241–243
8. Baetens R, Jelle PB, Gustavsen A (2011) Aerogel insulation for building applications: a state-of-the-art review. Energy Build 43 (4):761–769
9. Ackerman WC, Vlachos RF (2001) Use of surface treated aerogels derived from various silica precursors in translucent insulation panels. J Noncryst Solids 285(1):264–271
10. Ruben GC, Pekala RW (1995) High-resolution transmission electron microscopy of the nanostructure of melamine-formaldehyde aerogels. J Noncryst Solids 186(2):219–231
11. Nguyen MH, Dao LH (1998) Effects of processing variable on melamine–formaldehyde aerogel formation. J Noncryst Solids 225 (1):51–57
12. Meena AK, Mishra GK, Rai PK, Rajagopal C, Nagar PN (2005) Removal of heavy metal ions from aqueous solutions using carbon aerogel as an adsorbent. J Hazard Mater 122(1):161–170
13. Kłonkowski AM, Grobelna B, Widernik T, Jankowska-Frydel A, Mozgawa W (1999) The coordination state of copper(II) complexes anchored and grafted onto the surface of organically modified silicates†. Langmuir 15(18):5814–5819
14. Motahari S, Nodeh M, Maghsoudi K (2015) Absorption of heavy metals using resorcinol formaldehyde aerogel modified with amine groups. Desalin Water Treat 1–12. https://doi.org/10.1080/19443994.2015.1082506
15. Geng B, Wang H, Wu S, Ru J, Tong C, Chen Y, Liu H, Wu S, Liu X (2017) Surface-tailored nanocellulose aerogels with thiol-functional moieties for highly efficient and selective removal of Hg(II) ions from water. ACS Sustain Chem Eng 5(12):11715–11726. https://doi.org/10.1021/acssuschemeng.7b03188
16. Aydın A, İmamoğlu M, Gülfen M (2010) Separation and recovery of gold(III) from base metal ions using melamine–formaldehyde–thiourea chelating resin. J Appl Polym Sci 107 (2):1201–1206

17. Yong Z, Zhu J, Ren H, Bi Y, Shi X, Wang B, Lin Z (2017) A novel starch-enhanced melamine-formaldehyde aerogel with low volume shrinkage and high toughness. J Porous Mater 24(5):1303–1307
18. Yong Z, Zhu J, Ren H, Bi Y, Lin Z (2017) Synthesis and properties of melamine–starch hybrid aerogels cross-linked with formaldehyde. J Sol–Gel Sci Technol 83(1):1–9
19. Birinci G, Mustafa A, Osman A (2009) Separation and recovery of palladium(II) from base metal ions by melamine-formaldehyde-thiourea (MFT) chelating resin. Hydrometallurgy 95(1):15–21
20. Ni C (2010) Synthesis and adsorption properties of chelating resin from thiourea and formaldehyde. J Jingzhou Teach Coll 82 (13):3127–3132
21. Nalwa HS, Vasudevan P (1981) Electrical properties of thiourea-formaldehyde condensates. Eur Polym J 17(2):145–149
22. Gülfen M (2008) Separation and recovery of silver(I) ions from base metal ions by melamine-formaldehyde-thiourea (MFT) chelating resin. Sep Sci Technol 43(2):376–388